TWMS J. App. and Eng. Math. V.16, N.7, 2026, pp. 865-883

A LOCAL FRACTIONAL NON-STANDARD FINITE DIFFERENCE SCHEME FOR FRACTAL LWR MODEL OF TRAFFIC FLOW

B. POKHRIYAL[1*], P. GOSWAMI[1], K. KUMAR[1], §

Abstract. In this paper, a non-standard local fractional Crank-Nicolson finite difference scheme is proposed to determine an approximation to the solutions of the fractal LWR traffic flow model. The scheme is found to be consistent and unconditionally stable. In addition, Lax's equivalence theorem is used to guarantee the scheme's convergence. The suggested approach is validated by discussing a few exemplary cases and associated simulations. The acquired numerical solutions demonstrate how traffic density changes dynamically across time and space. The outcomes obtained with the suggested non-standard finite difference (NSFD) method demonstrate its effectiveness in numerically solving the problem of fractal traffic flow.

Keywords: Local fractional calculus, numerical scheme, non-standard finite difference scheme, Crank-Nicolson method, traffic flow model.

AMS Subject Classification: 35R11.

1. Introduction

The issue of traffic congestion has garnered significant attention from researchers and scientists in recent years. A wide range of traffic models have been proposed in recent decades to investigate the intricate phenomena. The continuum model and continuous functions effectively explain the traffic flow. The ways in which flow, density, and velocity—the three main variables interact are necessary for a more accurate depiction of traffic flow. Lighthill, Whitham, and Richards's (LWR) studies were the foundation for this approach [1, 2]. Numerous authors have examined the LWR model, including Daganzo [3], Zhang [4], Li [5], Gasser [6], Awetal [7], Bellomo and Coscia [8], and Bellomo et al. [9]. This model requires two key presumptions, which use homogeneity criteria to analyse traffic dynamics across a unidirectional route: the existence of an established flow-density relation and vehicle conservation. The LWR technique ideally uses the continuity equation and the assumption of a speed-density equilibrium relationship to simulate traffic flow and

[1] Dr B. R. Ambedkar University Delhi, Delhi-110006, India.
e-mail: pokhriyalbhawna17@gmail.com; ORCID 0009-0000-4868-7049.
e-mail: pranaygoswami83@gmail.com; ORCID 0000-0003-1205-1975.
e-mail: kranti31lu@gmail.com; ORCID 0000-0002-6361-8786.
* Corresponding author.
§ Manuscript received: April 15, 2025; accepted: August 01, 2025.
TWMS Journal of Applied and Engineering Mathematics, Vol.16, No.7;

depict traffic patterns.

Numerous studies were conducted in various scientific and engineering domains to ascertain the fractal framework found in nature, starting from Mandelbrot [10]. Many researchers, including Erramilli et al. [11], Lam and Wornell [12], Shang et al. [13], and Li et al. [14], have found that traffic networks share geometric similarities. The nondifferentiable phenomena were recently addressed using the local fractional calculus proposed in [15, 16, 17]. For instance, the diffusion and Helmholtz equations in the context of local fractional derivatives (LFDs) were published in [18]. Jafari et al. [19] have solved the n-Generalized KdV equation by local fractional homotopy analysis method. Analytical Solutions for a Generalized Nonlinear Local Fractional Bratu-Type Equation in a Fractal Environment have been identified by G. Alhamzi et al. [20, 21]. A new generalized fractional derivatives have been intoduced by S. M. Elnady et al. [22] which expands the potential applications by introducing new functions and unifying current fractional derivatives. In contrast, local fractional equations of Navier-Stokes were put forth in [16]. In [23], the fractal equations of Maxwell were put out. In [24], equations for nonhomogeneous heat with LFDs were investigated. The classical conservation law is not applicable when the physical quantity of density or speed governing vehicle traffic flow on the fractal network is a nondifferentiable function with time and space defined on Cantor sets. The work of Wang et al. [25] discusses the fractal or local fractional dynamic traffic flow model according to the law of local fractional conservation to figure out the problem mentioned above. The following describes the dynamic LWR traffic flow framework incorporating LFDs that has been modified fractally about local fractional or fractal calculus and governed by conservation laws

$$\frac{\partial^{\sigma}}{\partial \tau^{\sigma}} \wp(\varpi, \tau) + \kappa \frac{\partial^{\sigma}}{\partial \varpi^{\sigma}} \wp(\varpi, \tau) = \wp(\varpi, \tau), \; 0 < \sigma \leq 1, \tag{1}$$

along with the initial and boundary conditions

$$\wp(\varpi, 0) = g(\varpi), \; 0 < \varpi \leq L, \tag{2}$$

$$\wp(0, \tau) = h_1(\tau), \; \wp(L, \tau) = h_2(\tau), \; \tau > 0, \tag{3}$$

with constant κ and source term $\wp(\varpi, \tau)$ and σ represents local fractional order of derivative.

Fractals are irregular geometrical formations that do not alter as their shapes are magnified or when the magnification level increases. In addition to pertinent prospective applications in traffic flow problems and techniques, fractal theory applications can be observed in many streams. Fractal alteration of traffic flow techniques, including crash examination, travel-time credibility, and ramp metering, can impact future research paths. The Fractal theory yields more accurate performance measurement estimations than standard derivatives. Consequently, fractal theory may be a more useful method for calculating the flow of traffic over brief periods of time. Further, the fractional calculus is used to address a range of non-differentiable problems that emerge in complex systems of real-world events. The non-differentiability that arises in the fields of science and engineering was especially well-simulated by fractional ordinary or partial differential equations. Differentiation and integration of functions based on fractal sets are generalised in local fractional calculus, often known as fractal calculus. The problems involving non-differentiability of functions are not well modelled by the classical derivatives. Furthermore, fractal domains like the cantor set lack differentiability. Local fractional derivatives are used to solve the problem that arises with non-differentiable functions. Wang et al.[25] first examined the dynamical behaviour of the Cauchy form of linear and nonlinear fractal LWR traffic flow models within the constraints of fractal conservation laws. The entropy criteria for the fractal

version of the LWR model were constructed by Guo et al. [26] using the local fractional variational iteration method (LFVIM). The local fractional LWR (LFLWR) model has been studied using several local fractional analytical techniques, such as LFVIM, fractal Laplace decomposition method [27], local fractional approach of series expansion, LFVIM, and a computational hybrid strategy [28].
The nonlinear LFLWR framework of traffic flow is then investigated and expressed as

$$\frac{\partial^\sigma}{\partial\tau^\sigma}\wp\left(\varpi,\tau\right)+\varphi\left(\wp\right)\frac{\partial^\sigma}{\partial\varpi^\sigma}\wp\left(\varpi,\tau\right)=\wp\left(\varpi,\tau\right),\ 0<\sigma\leq 1, \tag{4}$$

along with the initial condition

$$\wp\left(\varpi,0\right)=g\left(\varpi\right),\ 0<\varpi\leq L, \tag{5}$$

and boundary conditions

$$\begin{cases}\wp\left(0,\tau\right)=h_1\left(\tau\right)\\ \wp\left(L,\tau\right)=h_2\left(\tau\right)\end{cases},\ \tau>0, \tag{6}$$

where φ is a function of density $\wp$, $g\left(\varpi\right)$ denotes a non differentiable function of space and $h_1\left(\tau\right)$ and $h_2\left(\tau\right)$ represent non differentiable function of time. The model mentioned above has been solved analytically and LFVIM and local fractional Laplace VIM have been used to obtain solutions [29]. As a first step, Goswami et al. [30] recently suggested a local finite difference approach to analyze the model. To investigate the solution of the fractal LWR model, the authors used a local fractional Crank-Nicolson scheme that utilised local fractional central difference to approximate local fractional derivatives.
This study aims to develop an effective non-standard finite difference (NSFD) method to solve the fractal traffic flow model and examine its dynamic behaviour. This paper proposes a local fractional non-standard Crank-Nicolson (NSCN) scheme, which is more accurate and efficient than the local fractional standard Crank-Nicolson (SCN) scheme. The results are compared by using numerical simulation, which clearly shows that fractal NSCN is more accurate than fractal SCN. The remaining sections are organized as follows: Section 2 deals with the preliminaries and notations that briefly detail the key concepts of local fractional calculus and the NSFD scheme. The local fractional NSCN scheme is described in Section 3. Sections 4 and 5 discuss the stability and consistency of the scheme. The numerical solution and simulation results are provided in Sections 6 and 7. The conclusion is drawn in Section 8.

2. Preliminaries and notations

The fundamental definitions of the local fractional calculus and the fractal NSFD discretisation are briefly covered in this section.

2.1. **Local fractional calculus.**

Definition 2.1. *[15] A function $\delta\left(\varpi\right)$, $\varpi\in\left(b,c\right)$ is called local fractional or fractal continuous (LFC) at $\varpi=\varpi_0$ in $\left(e,f\right)$ if*

$$\left|\delta\left(\varpi\right)-\delta\left(\varpi_0\right)\right|<e^\sigma,\ 0<\sigma\leq 1, \tag{7}$$

given, $\left|\varpi-\varpi_0\right|<f$, for $e,f>0$. If this follows for all $\varpi\in\left(b,c\right)$ then $\delta\left(\varpi\right)$ is called LFC on $\left(b,c\right)$ and is expressed as $\delta\left(\varpi\right)\in C_\sigma\left(b,c\right)$.

Definition 2.2. *[15] The local fractional or fractal derivative of function $\delta\left(\varpi\right)\in C_\sigma\left(b,c\right)$ at $\varpi=\varpi_0$ is read as*

$$D_\varpi^\sigma\delta\left(\varpi_0\right)=\delta^\sigma\left(\varpi_0\right)=\frac{d^\sigma}{d\varpi^\sigma}\delta\left(\varpi_0\right)=\lim_{\varpi\to\varpi_0}\frac{\Delta^\sigma\left(\delta\left(\varpi\right)-\delta\left(\varpi_0\right)\right)}{\Delta\left(\varpi-\varpi_0\right)^\sigma}, \tag{8}$$

where

$$\Delta^{\sigma}\left(\delta\left(\varpi\right)-\delta\left(\varpi_{0}\right)\right)\cong\Gamma\left(1+\sigma\right)\left(\delta\left(\varpi\right)-\delta\left(\varpi_{0}\right)\right). \tag{9}$$

Definition 2.3. *[15] Let an interval $[b,c]$ be partitioned as (a_v, a_{v+1}), $v=0,1,\cdots,T-1$ and $a_T=f$ with $\Delta a_v = a_{v+1}-a_v$ and $\Delta a=\max\{\Delta a_0,\ \Delta a_1,...\}$, then, the fractal integral of $\delta(\varpi)$ in $[b,c]$ is read as*

$${}_{b}J_{c}^{\sigma}\delta\left(\varpi\right)=\frac{1}{\Gamma\left(1+\sigma\right)}\int_{b}^{c}\delta\left(a\right)\left(da\right)^{\sigma}=\frac{1}{\Gamma\left(1+\sigma\right)}\lim_{\Delta a\rightarrow0}\sum_{v=0}^{T-1}\delta\left(a_{v}\right)\left(\Delta a_{v}\right)^{\sigma}. \tag{10}$$

Definition 2.4. *The Gamma function $\Gamma(j)$ is read as*

$$\Gamma\left(j\right)=\int_{0}^{\infty}\kappa^{j-1}\exp\left(\kappa\right),\ \Re\left(j\right)>0. \tag{11}$$

Definition 2.5. *[28, 15] The expression for the Mittage Leffler, Sine, and Cosine functions in fractal space is*

$$E_{\sigma}\left(\varpi^{\sigma}\right)=\sum_{a=0}^{\infty}\frac{\varpi^{a\sigma}}{\Gamma\left(1+a\sigma\right)},\ 0<\sigma\leq1, \tag{12}$$

$$\sin_{\sigma}\left(\varpi^{\sigma}\right)=\sum_{a=0}^{\infty}\left(-1\right)^{a}\frac{\varpi^{(2a+1)\sigma}}{\Gamma\left(1+\left(2a+1\right)\sigma\right)},\ 0<\sigma\leq1, \tag{13}$$

$$\cos_{\sigma}\left(\varpi^{\sigma}\right)=\sum_{a=0}^{\infty}\left(-1\right)^{a}\frac{\varpi^{2a\sigma}}{\Gamma\left(1+2a\sigma\right)},\ 0<\sigma\leq1. \tag{14}$$

Theorem 2.1. *[31] (Generalized local fractional Taylor formula, (GLFTF))*
Let $\delta^{(v+1)\sigma}(\varpi)\in C_{\sigma}(b,c)$, then the GLFTF for δ is defined as

$$\delta\left(\varpi\right)=\sum_{v=0}^{s}\frac{\delta^{v\sigma}\left(\varpi_{0}\right)}{\Gamma\left(1+v\sigma\right)}\left(\varpi-\varpi_{o}\right)^{v\sigma}+\frac{\delta^{(m+1)\sigma}\left(\ell\right)}{\Gamma\left(1+\left(f+1\right)\sigma\right)}\left(\varpi-\varpi_{o}\right)^{(f+1)\sigma}, \tag{15}$$

for $v=0,1,\cdots,f$ and $0<\sigma\leq1$, with $b<\varpi_0<\ell<\varpi<c$, $\forall\varpi\in(b,c)$.
Similarly, for $\delta(\varpi,\tau)\in C_{\sigma}(E)$, $\frac{\partial^{s\sigma}}{\partial\varpi^{f\sigma}\varpi^{(f-k)\sigma}}\delta\in C_{\sigma}(E)$, the GLFTF for two variables is read as

$$\delta\left(\varpi,\tau\right)=\sum_{f=0}^{f}\sum_{k=0}^{k=f}\frac{1}{\Gamma\left(1+f\sigma\right)}\left(\varpi-\varpi_{0}\right)^{\sigma}\left(\tau-\tau_{0}\right)^{(f-k)\sigma}\frac{\partial^{f\sigma}}{\partial\varpi^{k\sigma}\partial\tau^{(f-k)\sigma}}\delta\left(\varpi_{0},\tau_{0}\right). \tag{16}$$

Theorem 2.2. *[32] (Lax's equivalence theorem) Stability is the necessary and sufficient condition for convergence for a well-posed initial boundary value problem with a consistent finite difference approximation.*

2.2. **Non-standard finite difference scheme.** The non-standard finite difference (NSF D) method was initially introduced by Mickens for ordinary differential equations (ODEs) or partial differential equations (PDEs) [33, 34, 35]. This section introduces some remarks about NSFD schemes. If at least one of the following criteria is met, a scheme is considered non-standard:

- It makes use of the non-local approximation.
- Non-negative functions are used for the discretisation of derivatives, which is not conventional.

One of the most elementary discretisation techniques is the forward Euler approach. This technique substitutes $\frac{\varpi(\tau+h)-\varpi(\tau)}{h}$ for the derivative term $\frac{d\varpi}{d\tau}$, where h is the step size. On the other side, this term is replaced by $\frac{\varpi(\tau+h)-\varpi(\tau)}{\phi(h)}$ in the Mickens scheme, where $\phi(h)$ represents continuous function with step size h and meets the requirements listed below:

$$\phi(h) = h + O\left(h^2\right),\ 0 < \phi(h) < 1,\ h \to 0. \tag{17}$$

Some instances of functions $\phi(h)$ that meet these requirements are [33]:

$$\phi(h) = h,\ \sinh h,\ e^h - 1,\ \frac{1 - e^{-ah}}{h},\ etc, ... \tag{18}$$

Note that using any of these $\phi(h)$ will yield the typical result for the first derivative when taking the lim $h \to 0$ to obtain the derivative.

$$\frac{d\varpi}{d\tau} = \lim_{h\to 0} \frac{\varpi(\tau + \phi_1(h)) - \varpi(\tau)}{\phi_2(h)} = \lim_{h\to 0} \frac{\varpi(\tau + h) - \varpi(\tau)}{h}. \tag{19}$$

Along with this substitution, any non-linear components in the differential equation are swapped out with

$$\varpi^2 \to \begin{cases} \varpi_n \varpi_{n+1} \\ \varpi_{n-1}\varpi_n \end{cases}, \quad \varpi\gamma \to \begin{cases} \varpi_n \gamma_{n+1} \\ \varpi_{n-1}\gamma_n \end{cases}. \tag{20}$$

It can be asserted that there is no suitable generic strategy for selecting the denominator function $\phi(h)$ or for selecting which nonlinear terms to substitute; instead, specific methods can be found in [33, 34].

3. Local fractional non-standard Crank-Nicolson scheme

The region chosen to solve the problem is divided into geometric-shaped meshes, and an approximation of the solution is produced using the nodes of each mesh. The local fractional Taylor series is utilised instead of derivatives to provide appropriate finite difference techniques for addressing differential equations. Consequently, the existing differential equation problem has been changed to one that involves solving an algebraic system of equations consisting of difference equations. Thus, the system of algebraic equations that has been established can be easily solved by applying one of the direct or iterative processes.

Consider the domain of the solution $[0, L] \times [0, \infty]$ is partitioned along the space domain into N equal sub-intervals. The uniform step sizes for the space and time variables are represented by $\Delta x = h$ and $\Delta t = k$, respectively, such that

$$\varpi_i = ih, \quad \tau^j = jk \quad i = 0, 1, \cdots, N \quad j = 0, 1, 2, \cdots, \tag{21}$$

And we indicate

$$\rho_i^j = \rho(\varpi_i, \tau_j), \quad i = 0, 1, \cdots, N \quad j = 0, 1, 2, \cdots, \tag{22}$$

where the local fractional partial differential equation (LFPDE) (4) at $(i, j)th$ mesh point is approximated by the exact solution of the finite difference equation, denoted by ρ. We can now approximate the local fractional derivative using the generalised local fractional Taylor series (16) and the Mickens discretisation scheme [33], yielding the local fractional non-standard forward difference (NSFwD) approximation as

$$\left.\frac{\partial^\sigma}{\partial\tau^\sigma}\rho(\varpi, \tau)\right|_{(i,j)} \approx \Gamma(1 + \sigma)\left(\frac{\rho(\varpi, \tau + \Delta\tau) - \rho(\varpi, \tau)}{\phi(k)^\sigma}\right), \tag{23}$$

and the local fractional non-standard central difference (NSCD) approximation is given as

$$\frac{\partial^{\sigma}}{\partial \varpi^{\sigma}} \rho(\varpi, \tau)\Big|_{(i,j)} \approx \Gamma(1+\sigma)\left(\frac{\rho(\varpi+\Delta\varpi, \tau)-\rho(\varpi-\Delta\varpi, \tau)}{2\phi(h)^{\sigma}}\right). \tag{24}$$

Now we discretized the model equation (4) by applying the mean of the local fractional NSCD approximation to the local fractional derivative in space at the jth and (J + 1)th time levels, as well as the local fractional NSFD approximation to the local fractional derivative in time at node location (i, j). Thus, the local fractional NSCN scheme is obtained as

$$\Gamma(1+\sigma)\left(\frac{\rho_i^{j+1}-\rho_i^j}{\phi(k)^{\sigma}}\right)+\frac{\Gamma(1+\sigma)}{2}\varphi\left(\rho_{i-1}^j\right)\left(\frac{\rho_{i+1}^{j+1}-\rho_{i-1}^{j+1}}{2\phi(h)^{\sigma}}+\frac{\rho_{i+1}^j-\rho_{i-1}^j}{2\phi(h)^{\sigma}}\right)=0, \tag{25}$$

where ϕ is the continuous function. Note that the standard discretisation can be obtained by putting $\phi(h) = h$ in (25). Thus, the discretisation (25) is the generalization of its standard counterpart. Furthermore, the denominator function $\phi(h)$ needs to meet the following consistency requirement

$$\phi(h) = h^{\sigma} + O(h^{r}),\ r > \sigma,\ h \to 0, \tag{26}$$

this guarantees that, as h approaches zero, the discrete approximation (25) will converge to the corresponding continuous derivative. A few instances of conditions that are met and used in the study are

$$\phi(h) = h^{\sigma},\ \sinh h^{\sigma},\ \frac{1-e^{-h\sigma}}{h^{\sigma}},\ e^{h\sigma}-1,\ etc\ldots \tag{27}$$

4. Stability analysis

In this part, we use the von Neumann or Fourier series technique [32] to establish the stability requirement of the proposed NSFD scheme (25).

We shift our notation from ρ_i^j to $\rho(ph, qk) = \rho_p^q$ and utilise the complex exponential version of the Fourier series, which is $\sum G_n e^{\frac{in\pi\varpi}{Y}}$, where $i = \sqrt{-1}$ and Y is the length of ϖ-interval. Thus, we may write

$$G_n e^{\frac{in\pi\varpi}{Y}} = G_n e^{\frac{in\pi ph}{(N-1)h}} = G_n e^{i\vartheta_n ph}, \tag{28}$$

where $\vartheta_n = \frac{n\pi}{(N-1)h}$ and $(N-1)h = Y$.

The initial value along $t = 0$ at mesh point (p, q) is provided as

$$\rho_p^0 = \sum_{n=0}^{N-1} G_n e^{i\vartheta_n ph},\ p = 0, 1, \cdots, N-1. \tag{29}$$

Since G_n is a constant and can be ignored, we only need to look at the propagation of one initial value, that is, $e^{i\vartheta ph}$. To investigate the term's propagation as τ rises, we replace

$$\rho_p^q = e^{i\vartheta\varpi}e^{\gamma\tau} = e^{i\vartheta ph}e^{\gamma qk} = e^{i\vartheta ph}\Omega^q, \tag{30}$$

in the NSFD equation (25), where $\Omega = e^{\gamma k}$ is the amplification factor and γ is a complex constant. Additionally, we suppose for convenience that $\varphi\left(\rho_i^j\right) = \eta_i^j = \eta$. Thus, we have

$$\begin{aligned} &2de^{i\vartheta ph}\Omega^{q+1}+\eta\left(e^{i\vartheta(p+1)h}\Omega^{q+1}-e^{i\vartheta(p-1)h}\Omega^{q+1}+e^{i\vartheta(p+1)h}\Omega^{q}-e^{i\vartheta(p-1)h}\Omega^{q}\right)\\ &-2de^{i\vartheta ph}\Omega^{q}=0, \end{aligned} \tag{31}$$

where $d = 2\left(\frac{\phi(h)}{\phi(k)}\right)^{\sigma}$, dividing the (31) by $e^{i\vartheta ph}\Omega^{q}$, we get

$$2d\Omega + \eta\left(e^{i\vartheta h}\Omega - e^{-i\vartheta h}\Omega + e^{i\vartheta h} - e^{-i\vartheta h}\right) - 2d = 0, \tag{32}$$

which yields

$$2d\left(\Omega - 1\right) + 2i\sin\vartheta h\left(\Omega + 1\right) = 0, \tag{33}$$

the condition for a finite difference scheme to be stable is $|\Omega| \leq 1$, and it can be seen that

$$|\Omega| = \left|\frac{r - i\sin\vartheta h}{r + i\sin\vartheta h}\right| \leq 1, \tag{34}$$

Hence, the local fractional NSCN finite difference scheme for the LFLWR model is unconditionally stable for every $d > 0$.

5. Consistency of the scheme

Assume Please assumehe LFPDE (4) is approximated by the finite difference equation $H_{i,j}\left(\rho\right) = 0$ at $(i,j)th$ mesh point, with ρ as the exact solution. Let $\wp$ indicatindicateact solution of the LFPDE that represents the LFLWR model (4), with initial and boundary conditions (5) and (6). At mesh point (i,j), the local truncation error is thus provided as

$$\mathrm{T}_{i,j} = H_{i,j}\left(\zeta\right). \tag{35}$$

Thus, from (25), we can write

$$H_{i,j}\left(\wp\right) = 4\left(\frac{\phi\left(h\right)}{\phi\left(k\right)}\right)^{\sigma} + \varphi\left(\wp_{i}^{j}\right)\left\{\wp_{i+1}^{j+1} - \wp_{i-1}^{j+1} + \wp_{i+1}^{j} - \wp_{i-1}^{j}\right\}, \tag{36}$$

with the use of GLFTF and the Mickens approximation, $H_{i,j}\left(\wp\right)$ may now be represented in terms of powers of $\phi(h)^{\sigma}$ and $\phi(k)^{\sigma}$ and local fractional partial derivatives of $\wp$ at point (ih, jk). Equation (36) therefore becomes

$$\begin{aligned} H_{i,j}\left(\wp\right) = {} & 4\frac{\phi(h)^{\sigma}}{\Gamma\left(1+\sigma\right)}\left(\frac{\partial^{\sigma}\wp}{\partial\tau^{\sigma}}\right)_{(i,j)} + 4\frac{\phi(h)^{\sigma}\phi(k)^{\sigma}}{\Gamma\left(1+2\sigma\right)}\left(\frac{\partial^{2\sigma}\wp}{\partial\tau^{2\sigma}}\right)_{(i,j)} + 4\frac{\phi(h)^{\sigma}\phi(k)^{2\sigma}}{\Gamma\left(1+3\sigma\right)}\left(\frac{\partial^{3\sigma}\wp}{\partial\tau^{3\sigma}}\right)_{(i,j)} \\ & + 4\varphi\left(\wp_{i}^{j}\right)\frac{\phi(h)^{\sigma}}{\Gamma\left(1+\sigma\right)}\left(\frac{\partial^{\sigma}\wp}{\partial\varpi^{\sigma}}\right)_{(i,j)} + \varphi\left(\wp_{i}^{j}\right)\frac{\phi(h)^{\sigma}\phi(k)^{\sigma}}{\Gamma\left(1+2\sigma\right)}\left(\frac{\partial^{2\sigma}\wp}{\partial\varpi^{\sigma}\partial\tau^{\sigma}}\right)_{(i,j)} \\ & + 4\varphi\left(\wp_{i}^{j}\right)\frac{\phi(h)^{3\sigma}}{\Gamma\left(1+3\sigma\right)}\left(\frac{\partial^{3\sigma}\wp}{\partial\varpi^{3\sigma}}\right)_{(i,j)} + 2\varphi\left(\wp_{i}^{j}\right)\frac{\phi(h)^{\sigma}\phi(k)^{2\sigma}}{\Gamma\left(1+3\sigma\right)}\left(\frac{\partial^{3\sigma}\wp}{\partial\varpi^{\sigma}\partial\tau^{2\sigma}}\right)_{(i,j)} = 0, \end{aligned} \tag{37}$$

which implies

$$\begin{aligned} \mathrm{T}_{i,j} = H_{i,j}\left(\wp\right) = {} & 4\frac{\phi(h)^{\sigma}}{\Gamma\left(1+\sigma\right)}\left\{\left(\frac{\partial^{\sigma}\wp}{\partial\tau^{\sigma}}\right)_{(i,j)} + \varphi\left(\wp_{i}^{j}\right)\left(\frac{\partial^{\sigma}\wp}{\partial\varpi^{\sigma}}\right)_{(i,j)}\right\} + 4\frac{\phi(h)^{\sigma}\phi(k)^{\sigma}}{\Gamma\left(1+2\sigma\right)} \\ & \times\left\{\left(\frac{\partial^{2\sigma}\wp}{\partial\tau^{2\sigma}}\right)_{(i,j)} + \varphi\left(\wp_{i}^{j}\right)\left(\frac{\partial^{2\sigma}\wp}{\partial\varpi^{\sigma}\partial\tau^{\sigma}}\right)_{(i,j)}\right\} + 2\frac{\phi(h)^{\sigma}\phi(k)^{2\sigma}}{\Gamma\left(1+3\sigma\right)} \\ & \times\left\{\left(\frac{\partial^{3\sigma}\wp}{\partial\tau^{3\sigma}}\right)_{(i,j)} + \varphi\left(\wp_{i}^{j}\right)\left(\frac{\partial^{3\sigma}\wp}{\partial\varpi^{\sigma}\partial\tau^{2\sigma}}\right)_{(i,j)}\right\}, \end{aligned} \tag{38}$$

since, $\phi\left(h\right)$ meets the following consistency requirement

$$\phi\left(h\right) = h^{\sigma} + O\left(h^{r}\right),\ r > \sigma,\ h \to 0, \tag{39}$$

Therefore, It is evident that as $h \to 0$ and $k \to 0$, $\mathrm{T_{i,j}} \to 0$. Hence, the local fractional NSCN scheme for the LFLWR model is consistent [32]. Further, Lax's equivalence theorem for convergence ensures that the suggested local fractional NSCN scheme is convergent since it satisfies all consistency and stability requirements.

6. Numerical solution and simulation

To assess the efficacy of the proposed non-standard scheme, we employ a few LFLWR models as examples for which the exact solution is known. At the nodal point (i, j), the absolute error (AE) is expressed as

$$AE = \left| \wp_{i,j}^{exact} - \rho_{i,j}^{approx} \right|. \tag{40}$$

Example 6.1. *Consider the LFLWR model as [36]*

$$\frac{\partial^\sigma}{\partial \tau^\sigma} \wp(\varpi, \tau) + \frac{\partial^\sigma}{\partial \varpi^\sigma} \wp(\varpi, \tau) = 0, \ 0 < \sigma \leq 1, \tag{41}$$

along with the initial condition

$$\wp(\varpi, 0) = \sinh_\sigma(\varpi^\sigma), \ 0 < \varpi \leq 1, \tag{42}$$

and boundary conditions

$$\begin{cases} \wp(0, \tau) = -\sinh_\sigma(\tau^\sigma) \\ \wp(1, \tau) = \sinh_\sigma(1^\sigma)\cosh_\sigma(\tau^\sigma) - \cosh_\sigma(1^\sigma)\sinh_\sigma(\tau^\sigma) \end{cases}, \ \tau > 0. \tag{43}$$

The problem has an exact solution as

$$\wp(\varpi, \tau) = \sinh_\sigma(\varpi^\sigma)\cosh_\sigma(\tau^\sigma) - \cosh_\sigma(\varpi^\sigma)\sinh_\sigma(\tau^\sigma). \tag{44}$$

By using the local fractional NSCN scheme (25) and selecting $\phi(h) = 1 - e^{h\sigma}$, the non-standard discretisation of (41) is given by

$$2d\rho_i^{j+1} + \rho_{i+1}^{j+1} - \rho_{i-1}^{j+1} = 2d\rho_i^j - \rho_{i+1}^j + \rho_{i-1}^j, \tag{45}$$

where $d = 2\left(\frac{1-e^{h\sigma}}{1-e^{k\sigma}}\right)^\sigma$.

Example 6.2. *Consider the LFLWR model [36]*

$$\frac{\partial^\sigma}{\partial \tau^\sigma} \wp(\varpi, \tau) + \frac{1}{2}\frac{\partial^\sigma}{\partial \varpi^\sigma} \wp(\varpi, \tau) = 0, \ 0 < \sigma \leq 1, \tag{46}$$

along with the initial condition

$$\wp(\varpi, 0) = E_\sigma(\varpi^\sigma), \ 0 < \varpi \leq 1, \tag{47}$$

and the boundary conditions

$$\begin{cases} \wp(0, \tau) = \cosh_\sigma(0.5\tau^\sigma) - \sinh_\sigma(0.5\tau^\sigma) \\ \wp(1, \tau) = E_\sigma(1^\sigma)\{\cosh_\sigma(0.5\tau^\sigma) - \sinh_\sigma(0.5\tau^\sigma)\} \end{cases}, \quad \tau > 0. \tag{48}$$

The problem has an exact solution as

$$\wp(\varpi, \tau) = E_\sigma(\varpi^\sigma)\cosh_\sigma(2\tau^\sigma) - E_\sigma(\varpi^\sigma)\sinh_\sigma(2\tau^\sigma). \tag{49}$$

By using the local fractional NSCN scheme (25) *and selecting* $\phi(h) = 1 - e^{h\sigma}$, *the non-standard discretisation of* (46) *is given by*

$$2d\rho_i^{j+1} + \frac{1}{2}\left(\rho_{i+1}^{j+1} - \rho_{i-1}^{j+1}\right) = 2d\rho_i^j - \frac{1}{2}\left(\rho_{i+1}^j - \rho_{i-1}^j\right), \tag{50}$$

where $d = 2\left(\frac{1-e^{h\sigma}}{1-e^{k\sigma}}\right)^\sigma$.

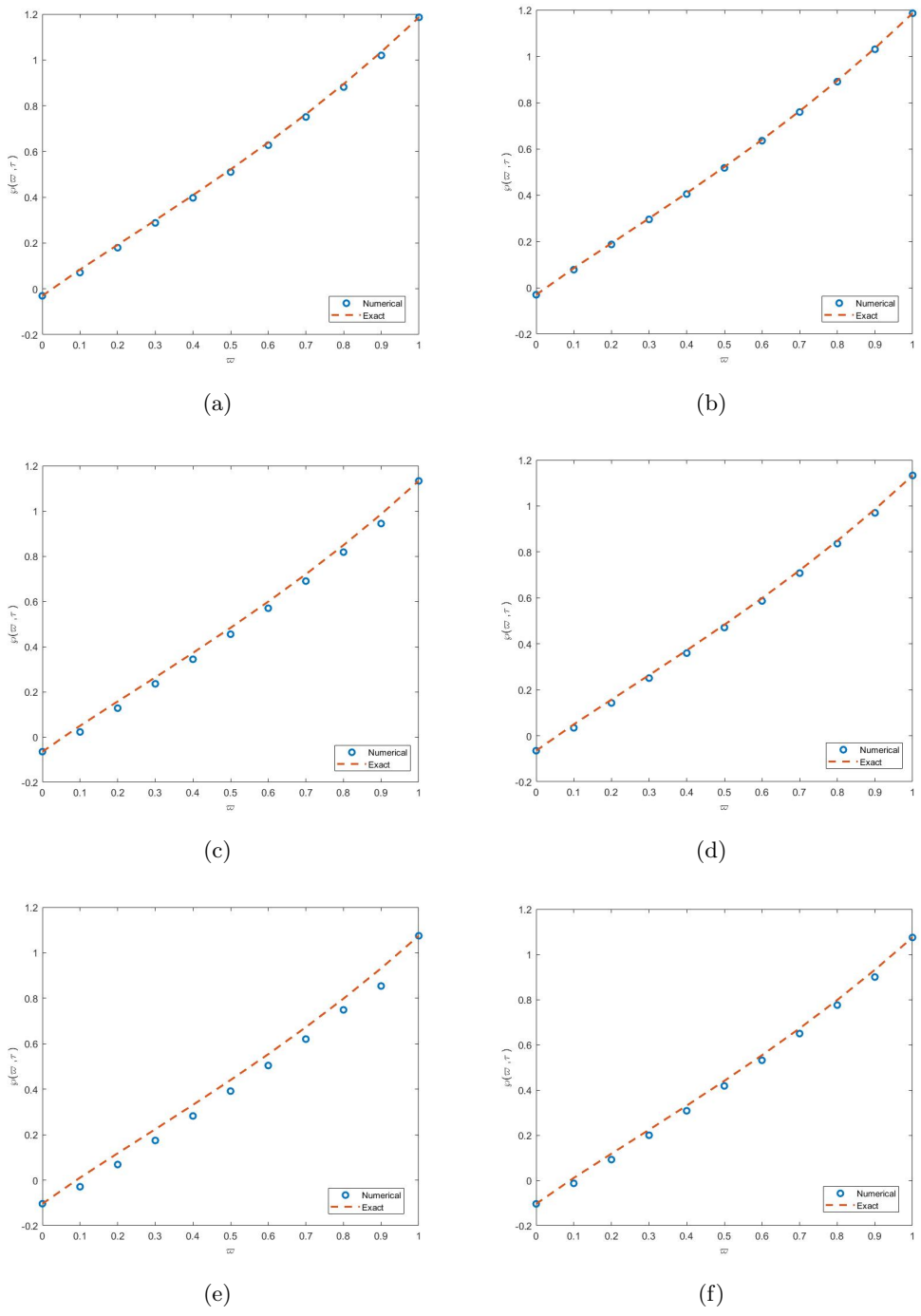

(a) (b) (c) (d) (e) (f)

FIGURE 1. ((a), (b)), ((c), (d)) and ((e), (f)) represent the comparison of numerical solution and exact solution by local fractional SCN and local fractional NSCN scheme at $t = 0.025$, $t = 0.050$ and $t = 0.075$, respectively, for $\sigma = 0.95$, $k = 0.0001$ and $h = 0.1$, for example 6.1

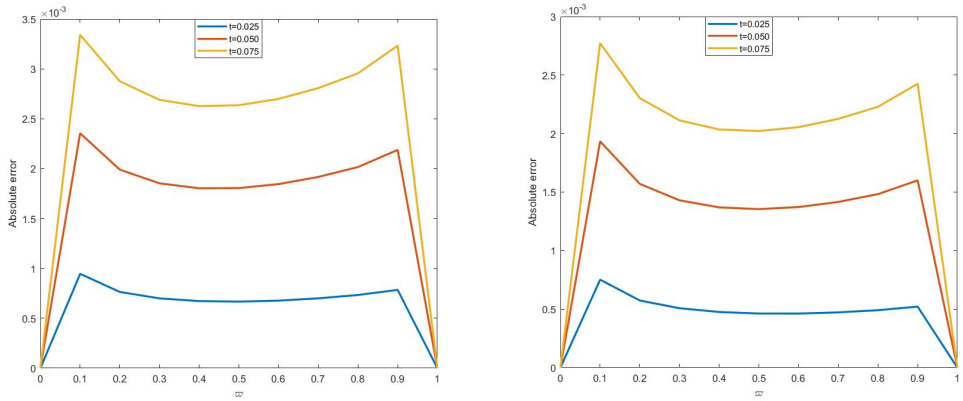

(a) (b)

FIGURE 2. (a) and (b) represent the AE between numerical solution and exact solution by local fractional SCN and local fractional NSCN scheme, respectively, at respective time step $\sigma = 0.95$, $k = 0.0001$ and $h = 0.1$, for example 6.1

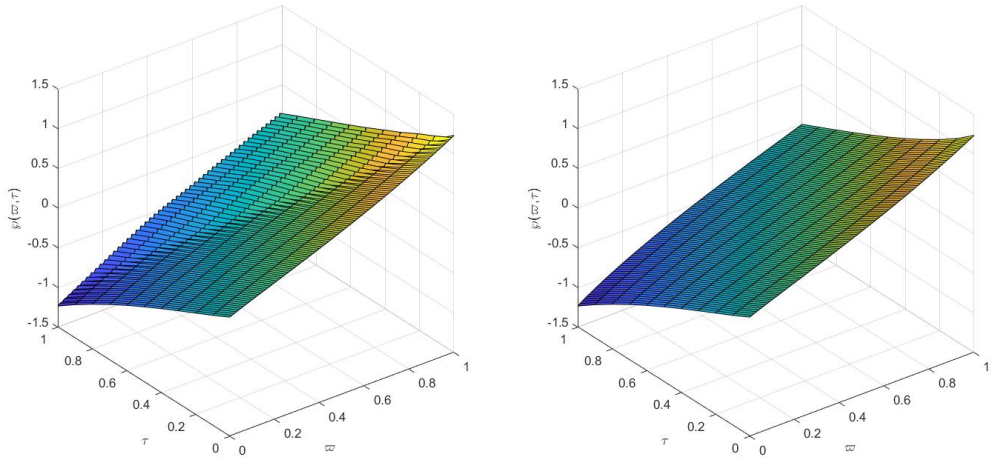

(a) (b)

FIGURE 3. (a) and (b) represent the numerical solution and exact solution surface, respectively, for $\sigma = 0.95$, $h = 0.01$ and $k = 0.01$, for example 6.1.

Example 6.3. *Consider the LFLWR model*

$$\frac{\partial^\sigma}{\partial \tau^\sigma} \wp(\varpi, \tau) + \wp(\varpi, \tau) \frac{\partial^\sigma}{\partial \varpi^\sigma} \wp(\varpi, \tau) = 0, \ 0 < \sigma \leq 1, \tag{51}$$

along with the initial condition

$$\wp(\varpi, 0) = \sinh_\sigma(\varpi^\sigma), \ 0 < \varpi \leq 1, \tag{52}$$

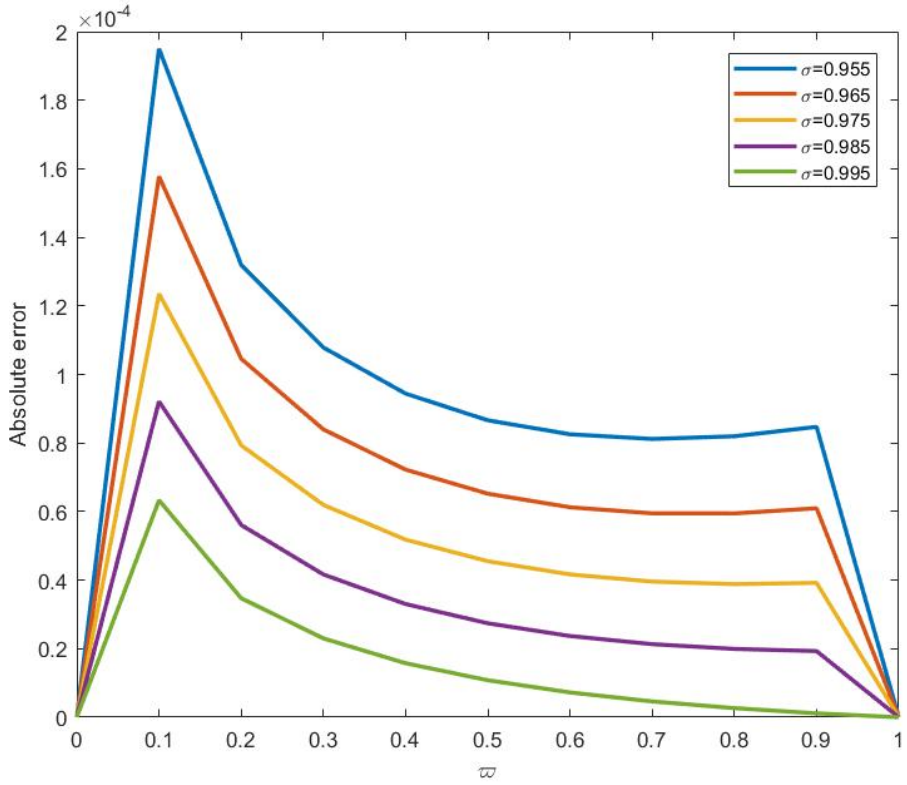

FIGURE 4. Comparison of AE between numerical solution and exact solution by local fractional NSCN scheme at $t = 0.025$ for $\sigma = 0.955, 0.965, 0.975, 0.985, 0.995$, $h = 0.1$ and $k = 0.0001$, for example 6.1.

TABLE 1. AE between numerical solution and exact solution by local fractional SCN and NSCN scheme at $t = 0.025$, 0.050 and 0.075, for $\sigma = 0.85$ at $k = 0.0001$ and $h = 0.1$, for example 6.1

SCN (at t=0.025) (10^{-3})	NSCN (at t=0.025) (10^{-4})	SCN (at t=0.050) (10^{-3})	NSCN (at t=0.050) (10^{-3})	SCN (at t=0.075) (10^{-3})	NSCN (at t=0.075) (10^{-3})
0	0	0	0	0	0
0.1297	0.9125	0.5140	0.3975	0.3130	0.2355
0.0914	0.5394	0.4019	0.2880	0.2372	0.1616
0.0772	0.3945	0.3622	0.2473	0.2101	0.1337
0.0697	0.3080	0.3439	0.2260	0.1968	0.1184
0.0656	0.2528	0.3380	0.2153	0.1914	0.1099
0.0640	0.2158	0.3406	0.2118	0.1913	0.1057
0.0641	0.1919	0.3502	0.2138	0.1954	0.1048
0.0657	0.1775	0.3657	0.2202	0.2032	0.1065
0.0686	0.1704	0.3887	0.2315	0.2149	0.1106
0	0	0	0	0	0

and boundary conditions

$$\begin{cases} \wp(0,\tau) = -\sinh_\sigma(\tau^\sigma) \\ \wp(1,\tau) = \sinh_\sigma(1^\sigma)\cosh_\sigma(\tau^\sigma) - \cosh_\sigma(1^\sigma)\sinh_\sigma(\tau^\sigma) \end{cases}, \ \tau > 0. \tag{53}$$

The exact solution of the problem is given as

$$\wp(\varpi,\tau) = \sinh_\sigma(\varpi^\sigma)\cosh_\sigma(\tau^\sigma) - \cosh_\sigma(\varpi^\sigma)\sinh_\sigma(\tau^\sigma). \tag{54}$$

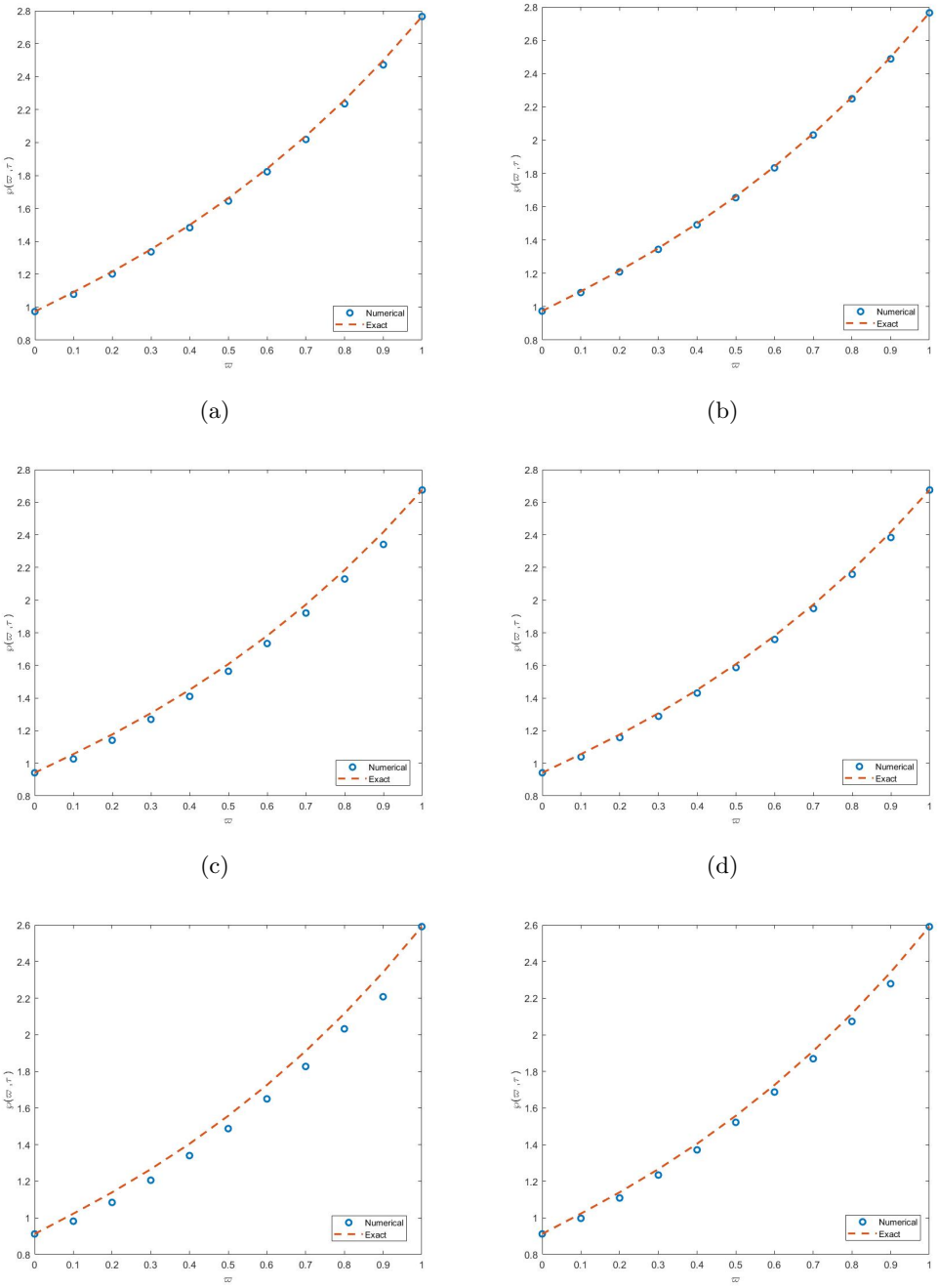

FIGURE 5. ((a), (b)), ((c), (d)) and ((e), (f)) represent the comparison of numerical solution and exact solution by local fractional SCN and local fractional NSCN scheme at $t = 0.025$, $t = 0.050$ and $t = 0.075$, respectively, for $\sigma = 0.95$, $k = 0.0001$ and $h = 0.1$, for example 6.2

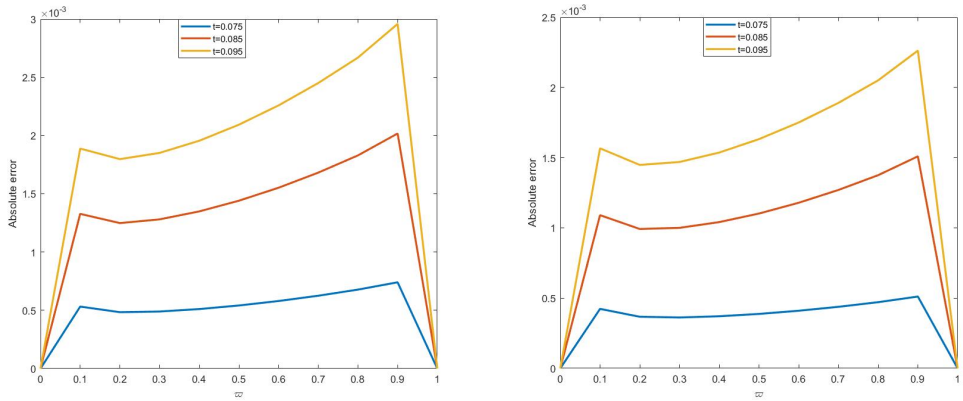

(a) (b)

FIGURE 6. (a) and (b) represent the AE between numerical solution and exact solution by local fractional SCN and local fractional NSCN scheme, respectively, at respective time step for $\sigma = 0.95$, $k = 0.0001$ and $h = 0.1$, for example 6.2

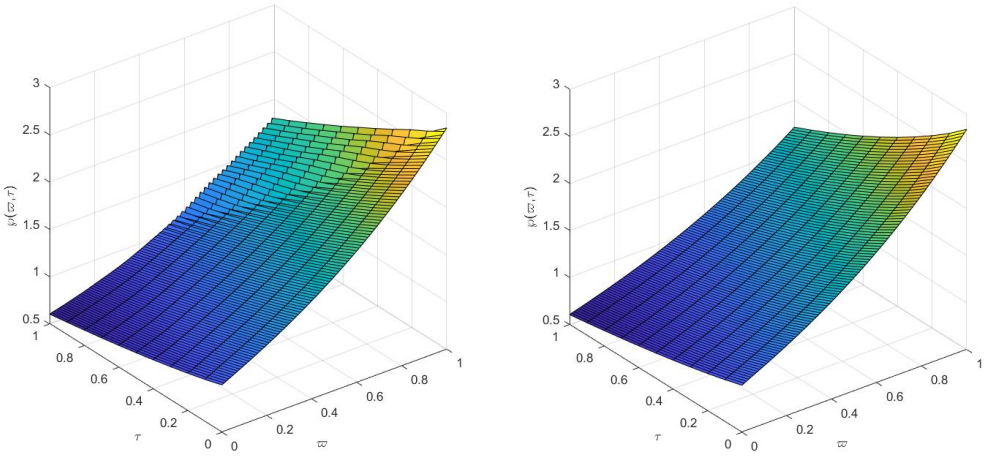

(a) (b)

FIGURE 7. (a) and (b) represent the numerical solution and exact solution surface, respectively, for $\sigma = 0.95$, $h = 0.01$ and $k = 0.01$, for example 6.2

By using the local fractional NSCN scheme (25) and selecting a suitable $\phi(h)$, the non-standard discretisation of (51) is given by

$$2d\rho_i^{j+1} + \rho_{i-1}^{j}\left(\rho_{i+1}^{j+1} - \rho_{i-1}^{j+1}\right) = 2d\rho_i^{j} - \rho_{i-1}^{j}\left(\rho_{i+1}^{j} - \rho_{i-1}^{j}\right), \tag{55}$$

where $d = 2\left(\frac{\phi(h)}{\phi(k)}\right)^{\sigma}$.

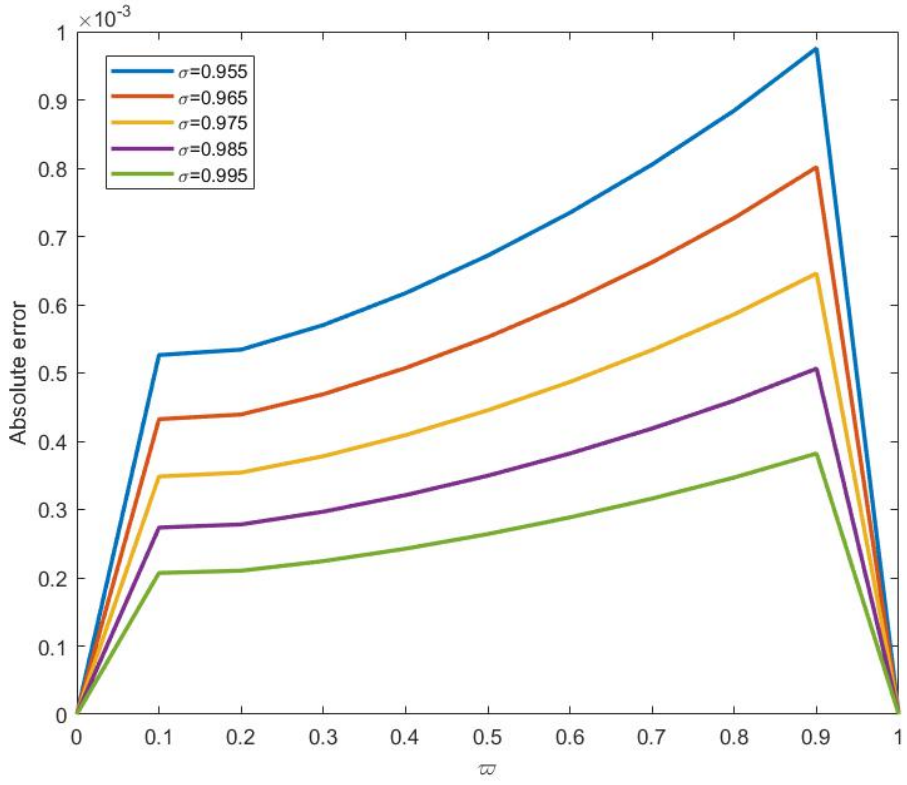

FIGURE 8. Comparison of AE between numerical solution and exact solution by local fractional NSCN scheme at $t = 0.025$ for $\sigma = 0.955, 0.965, 0.975, 0.985, 0.995$, $k = 0.0001$ and $h = 0.1$, for example 6.2

TABLE 2. AE between numerical solution and exact solution by local fractional SCN and NSCN scheme at $t = 0.025$, 0.050 and 0.075, for $\sigma = 0.85$ at $k = 0.0001$, $h = 0.1$, for example 6.2

SCN (at t=0.025) (10^{-4})	NSCN (at t=0.025) (10^{-4})	SCN (at t=0.050) (10^{-3})	NSCN (at t=0.050) (10^{-3})	SCN (at t=0.075) (10^{-3})	NSCN (at t=0.075) (10^{-3})
0	0	0	0	0	0
0.7302	0.5154	0.1760	0.1327	0.2889	0.2238
0.5953	0.3059	0.1522	0.1058	0.2562	0.1864
0.5673	0.3163	0.1500	0.0994	0.2559	0.1797
0.5656	0.2900	0.1536	0.0979	0.2645	0.1808
0.5784	0.2750	0.1604	0.0992	0.2785	0.1863
0.6015	0.2671	0.1698	0.1023	0.2966	0.1950
0.6330	0.2641	0.1814	0.1069	0.3184	0.2063
0.6722	0.2651	0.1950	0.1128	0.3438	0.2201
0.7193	0.2693	0.2111	0.1201	0.3738	0.2367
0	0	0	0	0	0

7. SIMULATION RESULTS

Several numerical results illustrating the dynamic behaviors of the LFLWR model of fractal traffic flow (4) are presented in this section. We compare the numerical and exact solutions to confirm the effectiveness of the suggested local fractional NSFD scheme and it is found that the numerical and exact solutions correspond well. Figures 1 and 5

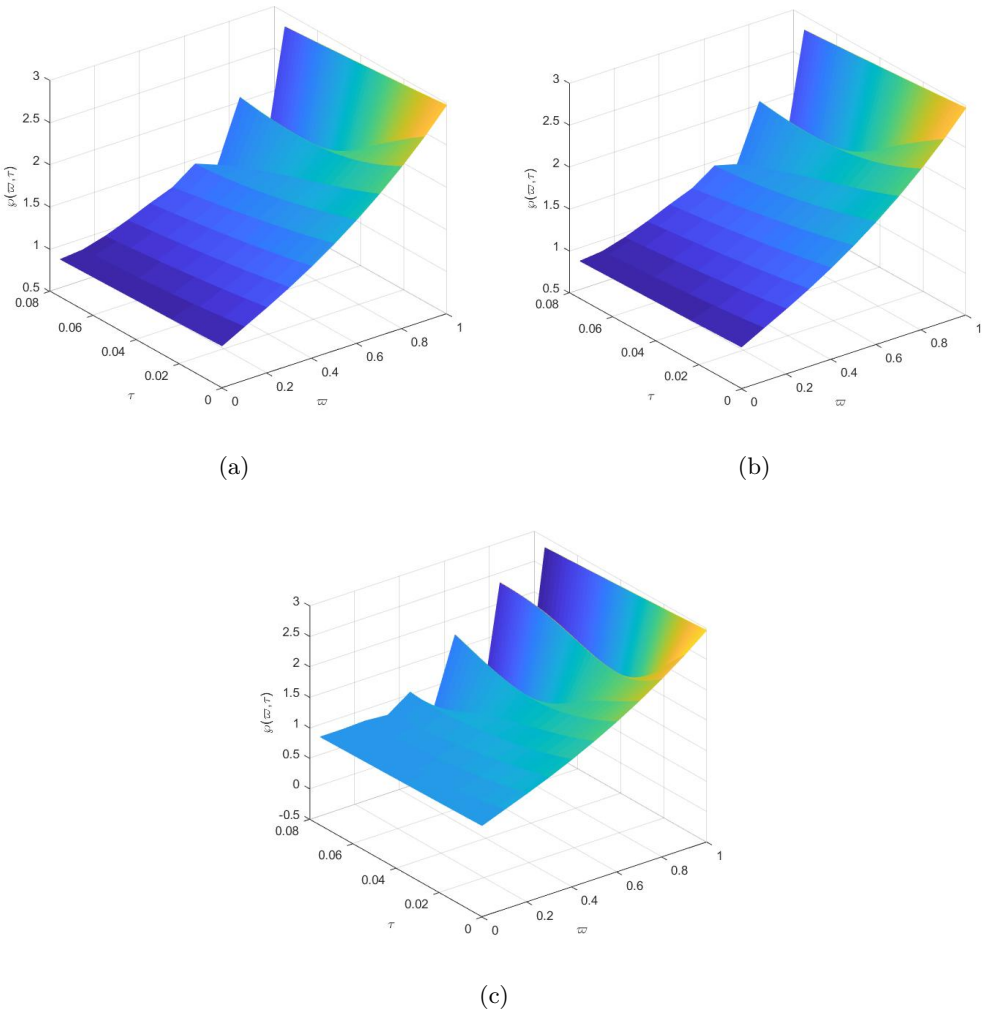

FIGURE 9. (a), (b) and (c) represent the numerical solution surface when is taken $\phi(h) = h^{\sigma}$, $1 - e^{h\sigma}$ *and* sinh h^{σ}, respectively, for $\sigma = 0.95$, $h = 0.01$ and $k = 0.01$, for example 6.3

demonstrate the approximate solutions in the fractal sense. Graphs (a) and (b) in Figure 1 represent the comparison of approximate and exact solutions using local fractional SCN and NSCN scheme at time step $t = 0.025$, graph (c) and (d) represent the comparison at time step $t = 0.050$ and graph (e) and (f) display the comparison among the solutions at time step $t = 0.075$. Furthermore, Figures 2 and 6 display the AE between the numerical and exact solutions using local fractional SCN and NSCN schemes at time steps $t = 0.025, 0.050$ and 0.075. It is evident from the simulations that the NSFD scheme gives more accurate results than the SFD scheme (see Tables 1 and 2). Figures 3 and 7 demonstrate the solution surfaces for approximate and exact solutions. The entire study of LWR model is conducted over a fractal space with fractal order of derivative σ. We compared the AE between the numerical solution and the exact solution using the NSFD scheme at the time step $t = 0.025$ for different $\sigma = 0.955$, 0.965, 0.975, 0.985 and 0.995 to examine the impact of fractal order (see Figures 4 and 8). Furthermore, we use SFD and NSFD schemes to

simulate the solution numerically surfaces to illustrate the differences; in addition, we incorporate different $\phi(h)$ to observe the impact on solution surfaces (see Figure 9).

8. Conclusion and future direction

This paper proposes a local fractional NSCN finite difference technique to estimate the approximation to solutions of the LFLWR model. The local fractional NSCN scheme can converge because its stability and consistency are well-established. To demonstrate the efficacy of the method, several examples have been provided along with their numerical simulations. The efficiency of the suggested NSFD scheme is first demonstrated by comparing its results with the results of the SFD scheme with local fractional derivatives (refer Tables 1 and 2). Additionally, a comparison between the exact solutions of the LFLWR model and the numerical solutions using the NSFD scheme reveals that the model's numerical solutions are convergent to the exact solution. The usefulness and efficiency of the suggested method, which can be applied to a range of non-linear LFLWR traffic flow models, have been demonstrated by this comparison. MATLAB software is used to display the simulations. Moreover, the dynamic behaviour of the non-differentiable traffic density function over time is demonstrated by the numerical solutions generated by the NSFD method. The simulations demonstrate how the traffic density behaves differently at various time intervals (refer to Figures 1, 3, 5 and 7). These representations further demonstrate the effectiveness and utility of the proposed scheme by confirming a good agreement between numerical solutions and exact solutions.
In subsequent research, we will examine several non-linear LFLWR traffic flow models and use difference techniques to find numerical solutions. To obtain some fresh perspectives and insights, we will investigate the solution using real traffic statistics.

9. Declarations

Conflict of Interest. Researchers state that there are no conflicts of interest to report regarding the presented article.

Availability of data and material. Not applicable.

Authors' contribution. Conceptualization, Bhawna Pokhriyal and Pranay Goswami; Methodology, Bhawna Pokhriyal, Pranay Goswami, Kranti Kumar; Formal analysis, Bhawna Pokhriyal; Investigation, Bhawna Pokhriyal; Resources, Kranti Kumar; Writing – original draft, Bhawna Pokhriyal; Writing – review & editing, Pranay Goswami; Visualization, Bhawna Pokhriyal; Supervision, Pranay Goswami, Kranti Kumar.

Funding. Not applicable.

References

[1] Lighthill, M. J. and Whitham, G. B., (1955), On kinematic waves II. A theory of traffic flow on long crowded roads, Proceedings of the Royal Society of London, Series A, Mathematical and Physical Sciences, 229(1178), 317–345.
[2] Richards, P. I., (1956), Shock waves on the highway, Operations Research, 4(1), 42–51.
[3] Daganzo, C. F., (1997), A continuum theory of traffic dynamics for freeways with special lanes, Transportation Research Part B: Methodological, 31(2), 83–102.
[4] Zhang, H. M., (2001), New perspectives on continuum traffic flow models, Networks and Spatial Economics, 1, 9–33.
[5] Li, T., (2001), L^1 stability of conservation laws for a traffic flow model., Electronic Journal of Differential Equations [electronic only] 2001(2001),14, pp. 1-18.

[6] Gasser, I., (2003), On non-entropy solutions of scalar conservation laws for traffic flow, ZAMM-Journal of Applied Mathematics and Mechanics/Zeitschrift f¨ur Angewandte Mathematik und Mechanik: Applied Mathematics and Mechanics, 83(2), 137–143.
[7] Aw, A., Klar, A., Rascle, M. and Materne, T., (2002), Derivation of continuum traffic flow models from microscopic follow-the-leader models, SIAM Journal on applied mathematics, 63(1), 259–278.
[8] Bellomo, N. and Coscia, V., (2005), First order models and closure of the mass conservation equation in the mathematical theory of vehicular traffic flow, Comptes Rendus Mecanique, 333(11), 843–851.
[9] Bellomo, N., Delitala, M. and Coscia, V., (2002), On the mathematical theory of vehicular traffic flow i: Fluid dynamic and kinetic modelling, Mathematical Models and Methods in Applied Sciences, 12(12), 1801–1843.
[10] Mandelbrot, B. B., (1982), The fractal geometry of nature, WH Freedman and Co., New York, 1(983), 1.
[11] Erramilli, A., Willinger, W. and Pruthi, P., (1994), Fractal traffic flows in high-speed communications networks, Fractals, 2(03), 409–412.
[12] Lam, W. M. and Wornell, G. W., (2001), Multiscale analysis and control of networks with fractal traffic, Applied and Computational Harmonic Analysis, 11(1), 124–146.
[13] Shang, P., Wan, M. and Kama, S., (2007), Fractal nature of highway traffic data, Computers & Mathematics with Applications, 54(1), 107–116.
[14] Li, M., Zhao, W. and Cattani, C., (2013), Delay bound: fractal traffic passes through network servers, Mathematical Problems in Engineering, 2013(1), 157636.
[15] Yang, X.-J., (2012), Advanced local fractional calculus and its applications.
[16] Yang, X.-J., Baleanu, D. and Tenreiro Machado, J., (2013), Systems of navier-stokes equations on cantor sets, Mathematical Problems in Engineering, 2013(1), 769724.
[17] Teodoro, G. S., Machado, J. T. and De Oliveira, E. C., (2019), A review of definitions of fractional derivatives and other operators, Journal of Computational Physics, 388, 195–208.
[18] Hao, Y.-J., Srivastava, H., Jafari, H. and Yang, X.-J., (2013), Helmholtz and diffusion equations associated with local fractional derivative operators involving the cantorian and cantor-type cylindrical coordinates, Advances in Mathematical Physics, 2013(1), 754248.
[19] Jafari, H., Prasad, J. G., Goswami, P. and Dubey, R. S., (2021), Solution of the local fractional generalized kdv equation using homotopy analysis method, Fractals, 29(05), 2140014.
[20] Alhamzi, G., Dubey, R. S., Alkahtani, B. S. T. and Saini, G., (2023), Analytical solutions for a generalized nonlinear local fractional bratu-type equation in a fractal environment, Fractal and Fractional, 8(1), 15.
[21] Alhamzi, G., Gouri, A., Alkahtani, B. S. T. and Dubey, R. S., (2024), Analytical solution of generalized bratu-type fractional differential equations using the homotopy perturbation transform method, Axioms, 13(2), 133.
[22] Elnady, S. M., El-Beltagy, M., Radwan, A. G. and Fouda, M. E., (2025), A generalized local fractional derivative with applications, Journal of Computational Physics, 530, 113903.
[23] Zhao, Y., Baleanu, D., Cattani, C., Cheng, D.-F. and Yang, X.-J., (2013), Maxwell's equations on cantor sets: a local fractional approach, Advances in High Energy Physics, 2013(1), 686371.
[24] Yang, A.-M., Cattani, C., Zhang, C., Xie, G.-N. and Yang, X.-J., (2014), Local fractional fourier series solutions for nonhomogeneous heat equations arising in fractal heat flow with local fractional derivative, Advances in Mechanical Engineering, 6, 514639.
[25] Wang, L.-F., Yang, X.-J., Baleanu, D., Cattani, C. and Zhao, Y., (2014), Fractal dynamical model of vehicular traffic flow within the local fractional conservation laws, Abstract and Applied Analysis, Vol. 2014, p. 635760.
[26] Guo, Y.-M., Zhao, Y., Zhou, Y.-M., Xiao, Z.-B. and Yang, X.-J., (2017), On the local fractional lwr model in fractal traffic flows in the entropy condition, Mathematical Methods in the Applied Sciences, 40(17), 6127–6132.
[27] Jassım, H., (2017), On approximate methods for fractal vehicular traffic flow, TWMS Journal of Applied and Engineering Mathematics, 7(1), 58–65.
[28] Kumar, D., Singh, J. and Baleanu, D., (2017), A hybrid computational approach for klein–gordon equations on cantor sets, Nonlinear Dynamics, 87, 511–517.
[29] Pokhriyal, B. and Goswami, P., (2023), A generalized local fractional lwr model of vehicular traffic flow and its solution, Mathematical Methods in the Applied Sciences, 46(18), 18899–18915.
[30] Goswami, P., Pokhriyal, B. and Kumar, K., (2024), A local fractional modified crank– nicolson scheme for fractal lwr model of traffic flow, International Journal of Geometric Methods in Modern Physics, p. 2440039.

[31] Yang, X.-J., (2011), Applications of local fractional calculus to engineering in fractal time-space: Local fractional differential equations with local fractional derivative, arXiv preprint arXiv, 1106.3010 .
[32] Smith, G. D., (1985), Numerical solution of partial differential equations: finite difference methods, Oxford University Press.
[33] Mickens, R. E., (1993), Nonstandard finite difference models of differential equations, world scientific.
[34] Mickens, R. E., (1999), Nonstandard finite difference schemes for reaction-diffusion equations, Numerical Methods for Partial Differential Equations: An International Journal, 15(2), 201–214.
[35] Mickens, R. E., (2003), A nonstandard finite difference scheme for a fisher pde having nonlinear diffusion, Computers & Mathematics with Applications, 45(1-3), 429–436.
[36] Kumar, D., Tchier, F., Singh, J. and Baleanu, D., (2018), An efficient computational technique for fractal vehicular traffic flow, Entropy, 20(4), 259.

Bhawna Pokhriyal has Master degree in Mathematics from University of Delhi. She has Senior Research Fellow position at Dr. B. R. Ambedkar University Delhi. Her study focusses on using local fractional derivatives with fractal domains to model traffic flow.

Dr. Pranay Goswami is an Associate Professor of Mathematics at the School of Liberal Studies, Dr. B.R. Ambedkar University Delhi, with a distinguished academic foundation comprising a B.Sc. (2003), M.Sc. (2005), and Ph.D. (2011) from the University of Rajasthan. He has an h-index of 22 and over 130 peer-reviewed international publications, his core expertise spans fractional differential and integral equations, geometric function theory, univalent functions, and applied mathematical modeling. His recent work prominently features advanced computational techniques, such as Haar wavelet and Chebyshev collocation methods, to solve complex nonlinear partial differential equations for real-world scientific applications.

Dr. Kranti Kumar is currently working as an Assistant Professor at the School of Liberal Studies, Dr. B.R. Ambedkar University Delhi, Delhi. He received PhD degree in Mathematics from Indian Institute of Technology Roorkee, Roorkee, India. His research interests include traffic flow modelling and prediction, traffic congestion modelling and prediction, noise pollution modelling, artificial neural networks, machine learning and deep learning.